Joint Time-of-Arrival Estimation for Coherent UWB Ranging in Multipath Environment With Multi-User Interference

Shangbo Wang, *Member, IEEE*, Guoqiang Mao, *Fellow, IEEE*, and J. Andrew Zhang, *Senior Member, IEEE*

***Abstract*—Time-of-Arrival (ToA) estimation becomes extremely challenging for ultra-wideband ranging systems in dense multipath environment with multiuser interference. In this paper, we propose a high accuracy joint ToA estimation (JToAE) algorithm, which can provide dominantly better performance than existing techniques. Based on the requirement of time synchronization among base stations, our proposed JToAE algorithm jointly exploits spatial information of each base station and the ToA of each multipath component of each received signal in ToA estimation. Our scheme is insensitive to the selection of the threshold, and does not require any additional information such as channel, noise power, preamble, or synchronization between transmitters and receivers. We also propose how to effectively distinguish the ToA of the first path of the desired user from the interfering signals in multi-user case without generating error propagation. The proposed JToAE is verified by extensive Monto Carlo simulation that is based on IEEE 802.15.4a channel models, and the simulation results indicate that even in low signal-to-noise ratio and multi-user case, our proposed technique can achieve significantly higher ranging accuracy compared to those in the literature in recent decades.**

***Index Terms*—Ultra Wide Band (UWB), Joint ToA Estimation (JToAE), Time of Arrival (ToA), Search-Back Algorithm (SbA), Multipath Component (MPC), IEEE 802.15.4a.**

I. Introduction

THERE is a growing demand for location awareness in communication networks. Highly accurate position information is of great importance in many commercial and military applications. UWB signal provides mainly two benefits for ranging and positioning applications. Firstly, UWB signal has extremely large bandwidth, which can lead to relatively fine time resolution and high possibility that at least some of the frequency components of the transmitted signal can penetrate through obstacles. Secondly, UWB signal has extremely low transmission power that poses tiny interference on NB (Narrow Band) systems and thus it can more easily coexist with other communication systems. The extremely high bandwidth and short pulses waveform help in reducing the effect of multipath interference and facilitate determination of ToA for burst transmission between the transmitter and corresponding receiver, which makes UWB a desirable solution for indoor positioning [1]. Therefore, UWB is considered to be an appropriate choice for the positioning applications that require relatively high accuracy and short-range coverage.

ToA/TDoA (Time of Arrival/Time Difference of Arrival) based algorithms are the most promising technique compared to RSS/AoA (Received Signal Strength/Angle of Arrival) based algorithms in UWB ranging systems because the aforementioned benefits can be fully explored in ToA/TDoA based UWB ranging systems. In ToA/TDoA based UWB ranging systems, multipath propagation introduces challenges for ToA estimation because of a large number of MPC (Multi-Path Components) and relatively long excess delays compared to the transmitted pulse duration. In the multipath environments, reflections from scatters in an environment arrive at receiver as replicas of the transmitted signal with various attenuation levels and delays [2]. Due to the antenna effect, i.e., non-uniform radiation, shadowing, the log-normal fading effect or multiuser transmission, the strongest path component may not be the first path component [2]. In dense multipath channels the first path is often not the strongest one, making ToA estimation challenging.

To tackle the problem, a number of ToA estimation techniques have been proposed in the recent decades. Existing methods can generally be classified into four categories: ML (Maximum Likelihood) approaches [3], MF (Matched Filter) based detectors [4], [5], energy based detectors [6]–[8] and machine-learning based approaches [9]–[11]. ML channel estimator can jointly deliver the ToA estimates and path amplitudes by maximizing the likelihood function. Theoretically, ML estimator is asymptotically efficient and it can achieve the CRLB (Cramer-Rao Lower Bound) in high SNR (Signal to Noise Ratio) region [12]. However, it is hard to be realized because of its high computational complexity. Energy based detectors cannot achieve high accuracy because it poses a square-law device on the received signal, which add the squared noise into the samples. Compared to energy based detectors, MF based detectors can provide better performance in high SNR region because it can maximize the received SNR. In low SNR region, however, MF is not able to deliver a satisfactory performance [12]. Another common drawback of the known MF based and energy based thresholding and search-back algorithms is that the estimation

Manuscript received June 29, 2018; revised January 24, 2019 and March 2, 2019; accepted April 24, 2019. Date of publication May 10, 2019; date of current version June 13, 2019. The associate editor coordinating the review of this manuscript and approving it for publication was Prof. Youngchul Sung. *(Corresponding author: Guoqiang Mao.)*

The authors are with the School of Electrical and Data Engineering, The University of Technology Sydney, Sydney, NSW 2007, Australia (e-mail: shangbo.wang@uts.edu.au; guoqiang.mao@uts.edu.au; andrew.zhang@uts.edu.au).

Digital Object Identifier 10.1109/TSP.2019.2916016

accuracy is too sensitive to the detection threshold. When the threshold is small, a high probability of early detection prior to the first path due to noise and interference is expected. On the other hand, if the threshold is large, we expect a low probability of detecting the first path [12]. Although some threshold selection approaches have been discussed in [4], [6]–[8], [13], thresholding algorithms are unable to deliver a satisfactory accuracy in low SNR region even if the optimal threshold is applied. The machine-learning based approaches have been already used to identify LoS (Line-of-Sight) and NLoS (Non-Line-of-Sight) in [9], [14]. They generally consist of data collection, feature extraction, model training and regression, which may have extremely high computational demand when the size of training data becomes large. In addition, the accuracy of machine-learning based approaches strongly rely on the selected model and its parameter optimization. Due to inappropriate model selection and the number of parameters, the model training may bring under-fitting or over-fitting problems which can lead to serious performance degradation.

In a multiuser UWB network, each user signal is transmitted through multi-paths and can interfere with each other at the receiver. Therefore, the observed strongest path component is not always the first path component of the desired user. Some literature focuses on studying the impact of MUI (Multi User Interference) [15] and mitigating MUI using a coherent receiver [6]. These papers utilize successive cancellation of users with maximum received energy where ToA of each user is iteratively estimated via finding the maximum value from the residual signal. The main problem of this approach is that the estimation accuracy relies strongly on the user-specific threshold, and the successive cancellation is an iterative algorithm and thus it causes error propagation problem.

Most existing ToA estimation techniques only rely on single received signal, that is, the signals received at other base stations are not utilized. In UWB positioning systems, the base stations are fixed and their locations are known. Such information can be exploited to further improve ToA estimation performance and reduce computational complexity. It is well-known that, in a line-of-sight (LoS) multipath channel environment, the target node location can be determined by intersecting a set of spheres, which are created by the location of each base station (center) and ToA of the first path (radius) of the desired user. Nevertheless, multipath components (MPCs) arrive later than the first path and thus they are unable to create a set of spheres intersecting at a unique point, and instead a point with Minimum Sum of Squared Distance (MSSD) from each sphere can be determined by the location of each base station and ToA of MPCs. It is obvious that MSSD should be equal to and larger than zero for the cases with first path and MPCs in perfect scenario (sufficient sampling rate, no Gaussian noise), respectively. Such difference can be utilized to distinguish the first path from MPCs.

Motivated by the intuition and aforementioned shortcomings of the existing estimation approaches, in this paper, we propose a joint ToA estimation approach (JToAE) that estimates ToA of the first path at each received signal by jointly considering the location information of each base station and ToA of each MPC. Due to utilization of spatial information of base stations, we can determine the most likely ToA at each received signal by comparing the MSSD from a group of spheres, rather than thresholding, without having to achieve synchronization between transmitters and receivers. More specifically, the following contributions are made in this paper:

- A novel JToAE is proposed that allows to explicitly incorporate the map information including location of each base station and MSSD into ToA estimation without having to know the number of MPCs for each user, estimate amplitude and delay for each MPC and achieve synchronization between transmitters and receivers.
- A low-complexity one path channel estimator is proposed and the relation between the time drift posed by window function and the expectation and variance of ToA estimates is investigated;
- We investigate the JToAE under consideration of MUI and show that our approach can be easily extended to the multi user case.
- Using IEEE 802.15.4a channel models, we demonstrate the superiority of the proposed scheme over the existing methods.

The rest of the paper is organized as follows: Section II reviews the related work. Section III proposes the system model. Section IV proposes the JToAE for the single user and multi user case, and analyzes its complexity. Section V verifies the proposed algorithm and compares its performance to the existing methods. Section VI concludes the study.

II. Related Work

A number of studies have been carried out to investigate UWB multipath fading channel, improve detection performance or analyze the error sources of the ToA estimation and its lower bound.

ML channel estimation, as the most classical method to estimate ToA of each MPC, has been extensively investigated in the last three decades. Win *et al.* gave a characterization of the UWB propagation channel from a communications theoretic view point and introduced ML channel estimator to estimate each MPC [3]. In [16], a GML (Generalized Maximum Likelihood) channel estimator is employed to estimate the channel parameters, which is in turn used to estimate the arrival time of the first path. However, the number of channels often cannot be determined within the search domain using the GML estimator. In addition, the channel parameter estimation is a laborious task whose computational complexity increases with the rise of the number of channels. In [17], a modification of the ToA algorithm to reduce the number of correlation computations in the DP (Direct Path) search process was proposed. A Minimum Mean Squared Error (MMSE) interpolator is employed to reduce computational complexity that acquires the missing samples between two adjacent samples caused by under-sampling process. However, MMSE interpolator requires the output signal of the correlator to be a wide sense stationary process, which, in the context of ToA estimation, is often a cyclo-stationary process in many cases.

D'Amico *et al.* proposed a structured approach to ToA estimation based on least squares (LS) techniques. A two-step procedure which first leads to a coarse estimate and then to a finer results was adopted [18]. Guvenc and Arslan proposed the Jump Back and Search Forward (JBSF) and the Serial Backward Search (SBS) and analyzed both theoretically and via simulations the trade-offs between the two kinds of search-back schemes based on the statistics of realistic channel models [19]. Guvenc and Sahinoglu introduced signal conditioning techniques based on a bank of cascaded multi-scale energy collection filters and wavelets. A more accurate detection can be achieved by exploiting correlations across multiple scales for edge and peak enhancements [20]. Dardari *et al.* proposed a practical ToA estimate scheme to mitigate both narrow-band and wide-band interference. The influence of interference on ToA estimation was evaluated [21]. Rabbachin *et al.* proposed a ML ToA estimation strategy based on energy detection approach utilizing a relatively long integration window [22]. Guvenc and Sahinoglu considered ToA estimation of the received signal based on symbol-rate samples, and the theoretical analysis and simulation of the performance of threshold based ToA estimation was proposed [23].

Savic *et al.* proposed kernel principal component analysis (kPCA), which projects the channel parameters onto a non-linear feature space and utilizes the projected parameters for ranging [10], [24]. Nguyen *et al.* utilized relevance vector machine technique to identify and mitigate NLoS signals [9]. The main problem of machine learning approaches is that they require fitting the empirical data prior to on-line data processing to optimize the model parameters and thus the computational complexity goes high when size of the empirical data becomes large.

Amigo *et al.* introduced and implemented successive cancellation of users with maximum received energy and concluded from the simulation results that the proposed algorithm can obtain smaller variance than the per-user ML estimator [25]. Kristem *et al.* proposed the MUI successive cancellation without having to know the TH (Time Hopping) sequences of the interfering users because of difficulty to acquire the TH sequences of all the interfering users [6]. The MUI successive cancellation estimates ToA of the desired user by finding the maximum value of a subtracted signal at each iteration and thus is subject to error propagation. Flury *et al.* designed two algorithms for reliable and robust synchronization of IR (Impulse Radio) UWB energy-detection receivers in the presence of MUI, which uses a correlation-based packet detection algorithm and a likelihood-based approach for timing acquisition, respectively [26]. Orthogonality of preamble compliant with the IEEE 802.15.4a is exploited to mitigate MUI and perfect synchronization is assumed [26].

The aforementioned review reveals that most existing studies have not incorporated both location information of base stations and ToA of each MPC of each received signal into detection procedure. Most literature are based on energy based detection which is very sensitive to the threshold selection and is lacking in achieving a satisfactory accuracy in low SNR region. In addition, most literature only proposed strategy for single user case, which may not be applicable in multi user case because of MUI.

III. System Model

We consider an UWB network scenario, in which *N* anchors have to localize *M* mobile stations using ToA measurements derived from the received signals of the mobile stations. We assume that the *N* anchors are connected to a central server and thus achieve the perfect time synchronization. The *N* anchors are fixed at the known locations of $\left(\boldsymbol{p_1} \cdots \boldsymbol{p_N}\right)$ and the *M* mobile stations are arbitrarily distributed over a region R, where $\boldsymbol{p_n}$ is the location vector of the *n*-th anchor consisting of *x* and *y* coordinates. The server is responsible for issuing commands and receiving signal from the *N* anchors. In this paper, we consider the IEEE 15.4a signal format and the information bits are modulated onto pulse train by PAM (Pulse Amplitude Modulation). Thus, the transmitted signal $s_m(t)$ from the *m*-th mobile station can be expressed by

$$s_m(t) = \sum_{i=0}^{I-1} d_{i,m} \sum_{k=0}^{K-1} p\left(t - iT_\mathrm{s} - kT_f - c_{k,m}T_\mathrm{c}\right) \quad (1)$$

where $p(t)$ is the pulse waveform with the pulse energy E_p, T_f is the frame duration, T_s is the symbol duration, T_c is the chip duration, $d_{i,m}$ represents the *i*-th data symbol of the *m*-th mobile station, $c_{k,m}$ represents the TH sequence allocated to the *k*-th frame of the *m*-th mobile station, *I* and *K* are the number of data symbols and frames, respectively.

The channel impulse response between the *m*-th mobile user and the *n*-th anchor can be modeled by the well-known tapped delay line expression

$$h_{mn}(t) = \sum_{l=0}^{L_{mn}-1} a_{l,mn}\delta\left(t - \tau_{l,mn}\right), \quad (2)$$

where $a_{l,mn}$ is the channel coefficient and $\tau_{l,mn}$ is the time delay of the *l*-th path, and L_{mn} is the number of channel paths between the *m*-th mobile and the *n*-th anchor. In this paper, we assume that we have a slow fading channel and the channel is time-invariant over several symbols, and thus L_{mn} is assumed to be a fixed number over several symbols. Parameter L_{mn} will be modeled according to the IEEE 802.15.4a channel model.

The received signal $r_n(t)$ at the *n*-th anchor consists of the desired signal, interference and the AWGN (Additive White Gaussian Noise) and thus can be expressed by

$$\begin{aligned} r_n(t) &= \int_{-\infty}^{\infty} s_j\left(\tau\right) h_{jn}(t-\tau)\mathrm{d}\tau + \sum_{m=1,m\neq j}^{M} I_{jm,n}(t) + w_n(t) \\ &= \sum_{i=0}^{I-1} d_{i,j} \sum_{l=0}^{L_{j,n}-1} a_{l,jn} \sum_{k=0}^{K-1} p\left(t - iT_s - kT_f - c_{k,j}T_\mathrm{c} - \tau_{l,jn}\right) \\ &\quad + \sum_{m=1,m\neq j}^{M} I_{mj,n}(t) + w_n(t) \end{aligned} \quad (3)$$

where $I_{mj,n}(t)$ and $w_n(t)$ represent the interference from other transmitters and the AWGN noise, respectively. For simplicity of expression, we neglect the information bit and only express the received signal for one symbol duration, and thus (3) can be simplified as

$$r_n(t) = \sum_{l=0}^{L_{j,n}-1} a_{l,jn} \sum_{k=0}^{K-1} p\left(t - kT_f - c_{k,j}T_{\mathrm{c}} - \tau_{l,jn}\right) + \sum_{m=1,m\neq j}^{M} \sum_{l=0}^{L_{mn}-1} a_{l,mn} \sum_{k=0}^{K-1} p\begin{pmatrix} t - kT_f \\ -c_{k,m}T_{\mathrm{c}} \\ -\tau_{l,mn} \end{pmatrix} + w_n(t) \quad (4)$$

We define the template signal as $T(t) = 1/\sqrt{E_{\mathrm{p}}}p\left(-t\right)$, where E_{p} is the pulse energy. After a convolution operation, the correlated signal $z_n(t)$ is given by

$$z_n(t) = \frac{1}{\sqrt{E_{\mathrm{p}}}} \sum_{l=0}^{L_{j,n}-1} a_{l,jn} \sum_{k=0}^{K-1} R_{\mathrm{p}} \begin{pmatrix} t - kT_f \\ -c_{k,j}T_{\mathrm{c}} \\ -\tau_{l,jn} \end{pmatrix} + R_{\mathrm{pw}}(t) + \frac{1}{\sqrt{E_{\mathrm{p}}}} \sum_{\substack{m=1 \\ m\neq j}}^{M} \sum_{l=0}^{L_{m,n}-1} a_{l,mn} \sum_{k=0}^{K-1} R_{\mathrm{p}} \begin{pmatrix} t - kT_f \\ -c_{k,m}T_{\mathrm{c}} \\ -\tau_{l,mn} \end{pmatrix} \quad (5)$$

where $R_{\mathrm{p}}(t)$ and $R_{\mathrm{pw}}(t)$ are the auto-correlation function of $p(t)$ and the cross correlation function of $w_n(t)$ and $T(t)$, respectively. The first and second term in (5) represent the correlated desired signal and correlated interference.

IV. Joint ToA Estimation

In this section, we start from the fundamental principle of JToAE for the single user case ($M = 1$, no interference), which will be extended to the multi user case in Subsection IV-C. We firstly briefly describe how to capture the correlation peaks at the received correlated signal using the search-back algorithm. Then, we describe how to fully exploit the location information of the base stations and ToAs of each captured peak to determine MSSD, and incorporate one-pulse ML channel estimator to estimate ToA.

Let us define $\hat{\boldsymbol{t}}_n = \left[\hat{t}_1 \ \hat{t}_2 \ \cdots \ \hat{t}_{D_n}\right]^{\mathrm{T}}, \hat{t}_1 < \cdots < \hat{t}_{D_n}$ as time displacement of the D_n captured peaks at the n-th receiver and can be estimated by [19]

$$\hat{\boldsymbol{t}}_n = \underset{t\in[0,t_{n,\max}]}{\arg} \left[|z_n(t)| \geq \frac{|v_{n,\max}|}{\sqrt{\eta}}\right] - \frac{T_{\mathrm{p}}}{2} \quad (6)$$

where $|.|$ is the absolute operation, η is a given threshold, T_{p} is the pulse duration, $v_{n,\max}$ and $t_{n,\max}$ are amplitude and time delay of the strongest correlation peak of the correlated signals within a certain threshold T_{th}, respectively. Note that $\hat{\boldsymbol{t}}_n$ obtained by (6) is the ToA of each captured peaks at the received signals, rather than the correlated signals. After filtering, the correlated signals spread out for T_{p} and thus the peak locations drift by $T_{\mathrm{p}}/2$. The search-back algorithm proposed in [19] utilized a predefined threshold ξ to search the samples arriving earlier than the strongest path. In this paper, we use the relative threshold η, with which the CDF (Cumulative Distribution Function) of first path being able to be captured via (6) can be obtained by an empirical simulation of IEEE 802.15.4a channel model.

If the first peak captured by (6) is considered to be the ToA of the first path, it may lead to a large estimation error even though for the single user case because the first peak detection strongly relies on the selection of η, that is, a larger η can lead to false detection to a noise peak and a smaller η can lead to missing detection of the actual ToA. In the multi user case, the error probability goes larger because of pulse aliasing from interferers. In our proposed JToAE, we select a relatively small η so that the actual ToA can be captured by $\hat{\boldsymbol{t}}_n$ in most cases.

We define the search space of JToAE by

$$\boldsymbol{S} = \left\{\left[\hat{t}_{d_1,1} \ \hat{t}_{d_2,2} \ \cdots \ \hat{t}_{d_N,N}\right] : \begin{matrix} d_1 \in [1\cdots D_1], \\ d_N \in [1\cdots D_N] \end{matrix}\right\} \quad (7)$$

where each element of $\boldsymbol{S}$ is a $1 \times N$ vector, which contains one randomly-selected captured peak delay for each receiver, $\hat{t}_{d_n,n}$ represents the d_n-th captured peak in $\hat{\boldsymbol{t}}_n$, $d_n, n = 1\cdots N$ is an arbitrary integer between 1 and D_n, the cardinality of $\boldsymbol{S}$ is $\prod_{n=1}^{N} D_n$ and the q-th element of $\boldsymbol{S}$ is expressed by $\boldsymbol{s_q}$. Our task is to estimate the ToA from each received signal, that is, to find the correct $\boldsymbol{s_q}$ from $\boldsymbol{S}$.

A. MSSD Determination for Each Element in $\boldsymbol{S}$

Suppose that the N receivers synchronize with each other and the transmitter is not synchronized with the receivers and transmits its signal at any arbitrary time. Let us define an unknown metric Δt as the time offset between the start time of the receivers and transmission time of the transmitter. Then, for q-th element of $\boldsymbol{S}$, the following relations can be obtained:

$$(x_n - \hat{x}_q)^2 + (y_n - \hat{y}_q)^2 = c^2\left(\hat{t}_{n,q} + \Delta t\right)^2, n = 1\cdots N \quad (8)$$

where c is the light speed, $\hat{t}_{n,q}$ is the time displacement of the captured peak at the n-th receiver for the q-th element of $\boldsymbol{S}$, x_n and y_n are the x coordinate and y coordinate of the n-th receiver, respectively, $\hat{x}_q$ and $\hat{y}_q$ are the x coordinate and y coordinate of the estimated point with MSSD from the group of spheres, respectively.

From (8), the following equation can be obtained:

$$\boldsymbol{H_q}\hat{\boldsymbol{d}}_{\boldsymbol{q}} = \boldsymbol{h_q} \quad (9)$$

where

$$\boldsymbol{H_q} = 2\begin{bmatrix} (x_2 - x_1) & (y_2 - y_1) & c^2\left(\hat{t}_{2,q} - \hat{t}_{1,q}\right) \\ (x_3 - x_2) & (y_3 - y_2) & c^2\left(\hat{t}_{3,q} - \hat{t}_{2,q}\right) \\ \vdots & \vdots & \vdots \\ (x_1 - x_N) & (y_1 - y_N) & c^2\left(\hat{t}_{1,q} - \hat{t}_{N,q}\right) \end{bmatrix}$$

$$\hat{\boldsymbol{d}}_{\boldsymbol{q}} = \begin{bmatrix} \hat{x}_q \\ \hat{y}_q \\ \Delta t \end{bmatrix}$$

$$\boldsymbol{h_q} = \begin{bmatrix} c^2\left(\hat{t}_{1,q}^2 - \hat{t}_{2,q}^2\right) - \left(x_1^2 - x_2^2\right) - \left(y_1^2 - y_2^2\right) \\ c^2\left(\hat{t}_{2,q}^2 - \hat{t}_{3,q}^2\right) - \left(x_2^2 - x_3^2\right) - \left(y_2^2 - y_3^2\right) \\ \vdots \\ c^2\left(\hat{t}_{N,q}^2 - \hat{t}_{1,q}^2\right) - \left(x_N^2 - x_1^2\right) - \left(y_N^2 - y_1^2\right) \end{bmatrix}$$

Then $\hat{\boldsymbol{d}}_{\boldsymbol{q}}$ can be obtained by

$$\hat{\boldsymbol{d}}_{\boldsymbol{q}} = \left(\boldsymbol{H_q}^{\mathrm{T}}\boldsymbol{H_q}\right)^{-1}\boldsymbol{H_q}^{\mathrm{T}}\boldsymbol{h_q} \quad (10)$$

Remark 1: Note that (9) only gives the two-dimensional case for simplicity of expression and thus equation (9) has a solution when rank of $\boldsymbol{H_q}$ is no less than three. Our method is also valid for three-dimensional case, in which the horizontal coordinate z_n should be incorporated and in such case, rank of $\boldsymbol{H_q}$ should be no less than four.

With $\hat{\boldsymbol{d}}_{\boldsymbol{q}}$, the MSSD can be determined by

$$MSSD_q = \sum_{n=1}^{N}\left(\sqrt{(x_n-\hat{x}_q)^2+(y_n-\hat{y}_q)^2}-c\left(\hat{t}_{q,n}+\Delta t\right)\right)^2 \tag{11}$$

Equation (11) is one of crucial metrics to determine the ToA. Intuitively, the *N* circles should intersect at a unique point for the case that $\boldsymbol{s_q}$ is the correct ToA vector, that is, $MSSD_q = 0$. With insufficient sampling rate, additive Gaussian noise and pulse overlapping, the correct ToA vector may suffer from a bias and thus $MSSD_q$ may be larger than zero. Let us define $MSSD_q$ by $A(\boldsymbol{s_q})$. The question then arises: can we detect the correct ToA vector by finding the minimum value of $A(\boldsymbol{s_q}), \boldsymbol{s_q} \in \boldsymbol{S}$? Note that the correct ToA vector is not the unique point that makes $A(\boldsymbol{s_q})$ zero, that means, $A(\boldsymbol{s_q})$ is a non-convex function with a non-strict global minimum at the correct ToA vector. To tackle the problem, a one-pulse ML channel estimator will be proposed in the next sub-section.

B. One-Pulse Maximum Likelihood Estimator (MLE)

The mean squared error (MSE) function can be expressed by

$$f(\boldsymbol{s_q}) = E\left\{\sum_{n=1}^{N}\int_{\hat{t}_{n,q}+\hat{\tau}_n-T_p/2}^{\hat{t}_{n,q}+\hat{\tau}_n+T_p/2}\begin{bmatrix} r_n(t)- \\ \hat{a}_n p\left(t-\hat{\tau}_n-\hat{t}_{n,q}\right)\end{bmatrix}^2 dt\right\} \tag{12}$$

where $\hat{a}_n$ and $\hat{\tau}_n$ are the estimated pulse amplitude and delay for the *n*-th base station given by (13) and (14), E is the expectation with respect to $w_n(t)$.

The conventional ML channel estimation is computationally intensive since it aims to estimate all separable MPCs through a convex optimization process. In this paper, we propose a one-pulse ML channel estimator which employs a window function to the received signal before channel estimation. One-pulse MLE has a low computational complexity and can estimate $\hat{a}_n$ and $\hat{\tau}_n$ by

$$\hat{\tau}_n = \underset{(\tilde{\tau}_n,\tilde{a}_n)}{\operatorname{argmin}}\int_{\hat{t}_{n,q}-T_p/2}^{\hat{t}_{n,q}+T_p/2}\left[r_n(t)-\tilde{a}_n p\left(t-\hat{t}_{n,q}-\tilde{\tau}_n\right)\right]^2 dt \tag{13}$$

and

$$\hat{a}_n = \int_{\hat{t}_{n,q}-T_p/2}^{\hat{t}_{n,q}+T_p/2} r_n(t)p\left(t-\hat{t}_{n,q}-\hat{\tau}_n\right)dt \tag{14}$$

where $\tilde{\tau}_n$ and $\tilde{a}_n$ represent the searched pulse delay and amplitude for the *n*-th receiver respectively. The function $f(\boldsymbol{s_q})$ denotes the sum of mean estimated squared error which is considered as another metric in this paper.

1) Estimation of Searched Pulse Delay and Amplitude: We firstly derive the optimum time delay $\hat{\tau}_n$ via (13). By applying a window function to the captured peak located at $\hat{t}_{n,q}$ and shifting the received signal in time domain by $\hat{t}_{n,q}$, we can rewrite (13) as

$$(\hat{\tau}_n,\hat{a}_n) = \underset{(\tilde{\tau}_n,\tilde{a}_n)}{\operatorname{argmin}}\left\{\begin{array}{l}\int_{-T_p/2}^{-T_p/2+\sigma_n}\begin{bmatrix} w_n(t)- \\ -\tilde{a}_n p(t-\tilde{\tau}_n)\end{bmatrix}^2 dt \\ +\int_{-T_p/2+\sigma_n}^{T_p/2}\begin{bmatrix} a_n p(t-\sigma_n)- \\ -\tilde{a}_n p(t-\tilde{\tau}_n) \\ +w_n(t)\end{bmatrix}^2 dt\end{array}\right\} \tag{15}$$

where σ_n and a_n are the time drift and the amplitude of the actual signal within the window function for the *n*-th base station, respectively, and $\sigma_n = t_{n,q} - \hat{t}_{n,q}$. The optimum $\hat{\tau}_n$ can be obtained by the first derivative of RHS (Right Hand Side) in (15) with respect to $\tilde{\tau}_n$ and setting it to zero:

$$0 = \frac{\partial F(\tilde{\tau}_n,\tilde{a}_n,\sigma_n,a_n)}{\partial\tilde{\tau}_n} = = 2\tilde{a}_n\begin{bmatrix}\int_{-T_p/2}^{T_p/2} w_n(t)p'(t-\tilde{\tau}_n)\,dt- \\ \tilde{a}_n\int_{-T_p/2}^{T_p/2} p(t-\tilde{\tau}_n)p'(t-\tilde{\tau}_n)\,dt+ \\ a_n\int_{-T_p/2+\sigma_n}^{-T_p/2} p(t-\sigma_n)p'(t-\tilde{\tau}_n)\,dt\end{bmatrix} \tag{16}$$

So it can be obtained

$$\tilde{a}_n\int_{-T_p/2}^{T_p/2}\begin{bmatrix} p(t-\hat{\tau}_n) \\ \times p'(t-\hat{\tau}_n)\end{bmatrix}dt = \int_{-T_p/2}^{T_p/2}\begin{bmatrix} w_n(t)\times \\ p'(t-\hat{\tau}_n)\end{bmatrix}dt + a_n\int_{-T_p/2+\sigma}^{-T_p/2}\begin{bmatrix} p(t-\sigma_n) \\ \times p'(t-\hat{\tau}_n)\end{bmatrix}dt \tag{17}$$

Similarly, the optimum $\hat{a}_n$ can be obtained by

$$0 = \frac{\partial F(\tilde{\tau}_n,\tilde{a}_n,\sigma_n,a_n)}{\partial\tilde{a}_n} = 2\begin{bmatrix}\tilde{a}_n\int_{-T_p/2}^{T_p/2} p^2(t-\tilde{\tau}_n)\,dt- \\ -\int_{-T_p/2}^{T_p/2} w_n(t)p(t-\tilde{\tau}_n)\,dt \\ -a_n\int_{-T_p/2+\sigma}^{T_p/2} p(t-\sigma_n)p(t-\tilde{\tau}_n)\,dt\end{bmatrix} \tag{18}$$

then

$$\hat{a}_n\int_{-T_p/2}^{T_p/2} p^2(t-\hat{\tau}_n)\,dt = \int_{-T_p/2}^{T_p/2} w_n(t)p(t-\hat{\tau}_n)\,dt + a_n\int_{-T_p/2+\sigma}^{T_p/2} p(t-\sigma_n)p(t-\hat{\tau}_n)\,dt \tag{19}$$

Combining with (17), the optimum $\hat{\tau}_n$ and $\hat{a}_n$ can be determined by

$$\frac{\int_{-T_p/2}^{T_p/2} w_n(t) p\left(t-\hat{\tau}_n\right) \mathrm{d}t + a_n \int_{-T_p/2+\sigma}^{T_p/2} p\left(t-\sigma_n\right) p\left(t-\hat{\tau}_n\right) \mathrm{d}t}{\int_{-T_p/2}^{T_p/2} p^2\left(t-\hat{\tau}_n\right) \mathrm{d}t} = \frac{\int_{-T_p/2}^{T_p/2} w_n(t) p'\left(t-\hat{\tau}_n\right) \mathrm{d}t + a_n \int_{-T_p/2+\sigma}^{T_p/2} p\left(t-\sigma_n\right) p'\left(t-\hat{\tau}_n\right) \mathrm{d}t}{\int_{-T_p/2}^{T_p/2} p\left(t-\hat{\tau}_n\right) p'\left(t-\hat{\tau}_n\right) \mathrm{d}t} \tag{20}$$

and

$$\hat{a}_n = \frac{\int_{-T_p/2}^{T_p/2} \left[w_n(t) p\left(t-\hat{\tau}_n\right)\right] \mathrm{d}t + a_n \int_{-T_p/2+\sigma_n}^{T_p/2} \left[p\left(t-\sigma_n\right) p\left(t-\hat{\tau}_n\right)\right] \mathrm{d}t}{\int_{-T_p/2}^{T_p/2} p^2\left(t-\hat{\tau}_n\right) \mathrm{d}t} \tag{21}$$

We can further show that the search pulse delay can be determined via Lemma 1:

Lemma 1: The searched pulse delay for the n-th receiver can be expressed by

$$\hat{\tau}_n \cong -\frac{R_{p'w}\left(\sigma_n\right) + \frac{a_n}{2} p^2\left(\frac{T_p}{2}-\sigma_n\right) - \frac{R_{pw}(\hat{\tau}_n) + a_n R_p(\hat{\tau}_n - \sigma_n)}{2} \times \left[p^2\left(\frac{T_p}{2}-\sigma_n\right) - p^2\left(-\frac{T_p}{2}-\sigma_n\right)\right]}{\left[a_n R_p\left(\hat{\tau}_n-\sigma_n\right) - a_n\right] \times p\left(\frac{T_p}{2}-\sigma_n\right) p'\left(\frac{T_p}{2}-\sigma_n\right) - a_n R_p\left(\hat{\tau}_n-\sigma_n\right) p\left(\frac{T_p}{2}+\sigma_n\right) p'\left(\frac{T_p}{2}+\sigma_n\right) + a_n \int_{-T_p/2+\sigma_n}^{T_p/2} p'^2\left(t-\sigma_n\right) \mathrm{d}t} \tag{22}$$

where $\cong$ stands for almost surely convergence, σ_n and a_n are the time drift and the amplitude of the actual signal within the window function for the n-th receiver, respectively, and $\sigma_n = t_{n,q} - \hat{t}_{n,q}$, σ_N^2 is the noise variance, $p'(t)$ is the first derivative of $p(t)$, $t_{n,q}$ is the actual n-th time displacement of $\boldsymbol{s_q}$.

Proof: See Appendix A. ■

It is non-trivial to directly solve $\hat{\tau}_n$ from (22) because of nonlinearity of $\hat{\tau}_n$ in the denominator and numerator of RHS of (22). Instead, we give the expectation and variance of $\hat{\tau}_n$, which can be used as a prerequisite of proving local minima at each $\boldsymbol{t}_{\text{stoa}}$, which stands for suspected ToA vector.

Lemma 2: The expectation and variance of $\hat{\tau}_n$ can be approximated by

$$E(\hat{\tau}_n) \approx \frac{-\frac{1}{2}p^2\left(-\frac{T_p}{2}-\sigma_n\right) - \sigma_n p\left(\frac{T_p}{2}-\sigma_n\right) p'\left(\frac{T_p}{2}-\sigma_n\right) + \sigma_n p\left(\frac{T_p}{2}+\sigma_n\right) p'\left(\frac{T_p}{2}+\sigma_n\right)}{-p\left(\frac{T_p}{2}+\sigma_n\right) p'\left(\frac{T_p}{2}+\sigma_n\right) + \int_{-T_p/2+\sigma_n}^{T_p/2} p'^2\left(t-\sigma_n\right) \mathrm{d}t} \tag{23}$$

and

$$var(\hat{\tau}_n) \approx \frac{\left[\begin{array}{c}\int_{-T_p/2-\sigma_n}^{T_p/2} p'^2(t) \mathrm{d}t \\ +\frac{1}{4}\left[p^2\left(\frac{T_p}{2}-\sigma_n\right) - p^2\left(-\frac{T_p}{2}-\sigma_n\right)\right]^2\end{array}\right] \sigma_N^2}{\left[\begin{array}{c} a_n \int_{-T_p/2+\sigma_n}^{T_p/2} p'^2\left(t-\sigma_n\right) \mathrm{d}t \\ -a_n p\left(\frac{T_p}{2}-\sigma_n\right) p'\left(\frac{T_p}{2}-\sigma_n\right)\end{array}\right]^2} \tag{24}$$

Proof: See Appendix B. ■

2) Non-Convexity of $f(\boldsymbol{s_q})$ and Its Multiple Local Minima: The function $f(\boldsymbol{s_q})$ is the MSE function depending on $\boldsymbol{t}_{\text{stoa}}$, $\hat{a}_n$ and $\hat{\tau}_n$. To additionally utilize the MSE metric delivered by the one-pulse MLE, we manage to prove the non-convexity of $f(\boldsymbol{s_q})$ and its ability to achieve the local minimum at each $\boldsymbol{t}_{\mathbf{stoa}}$, which is given by Theorem 1:

Theorem 1: Given the approximated searched pulse delay in (22) and its approximated expectation and variance in (23) and (24), the MSE function $f(\boldsymbol{s_q})$ is a non-convex function with the local minimum at each $\boldsymbol{t_{stoa}}$.

Proof: See Appendix C. ■

Remark 2: From the Lemma 1 to the Theorem 1, $t_{n,q}$ and $\hat{t}_{n,q}$ are respectively the q-th actual peak location and the estimated one by the search-back algorithm at the n-th receiver and $\sigma_n = t_{n,q} - \hat{t}_{n,q}$ is mainly introduced by the Gaussian noise and sampling time resolution. We can draw a conclusion from Theorem 1 that performance of the one-pulse MLE is influenced by the search-back algorithm; and the MSE function can achieve its local minimum at each actual peak.

Recall that $A(\boldsymbol{s_q})$ is a non-convex function with a non-strict global minimum at $\boldsymbol{t}_{\text{toa}}$, which stands for the correct ToA vector. Combining with Theorem 1, we can get the following theorem:

Theorem 2: With any positive numbers λ_1 and λ_2, the function

$$g(\boldsymbol{s_q}) = \lambda_1 A(\boldsymbol{s_q}) + \lambda_2 f(\boldsymbol{s_q})$$

has the unique global minimum at $\boldsymbol{t}_{\text{toa}}$.

Proof: From the definition of $A(\boldsymbol{s_q})$ and $f(\boldsymbol{s_q})$, it is clear that $A(\boldsymbol{t}_{\text{toa}}) = 0$, $f(\boldsymbol{t}_{\text{toa}}) = 0$ and $A(\boldsymbol{t}_{\text{stoa}}) \geq 0$, $f(\boldsymbol{t}_{\text{stoa}}) \geq 0$ for any $\boldsymbol{t}_{\text{stoa}}$. For each $\boldsymbol{t}_{\text{stoa}} \neq \boldsymbol{t}_{\text{toa}}$, $A(\boldsymbol{t}_{\text{stoa}})$ and $f(\boldsymbol{t}_{\text{stoa}})$ cannot achieve zero simultaneously. We can get $A(\boldsymbol{t}_{\text{stoa}}) > 0$ for each $\boldsymbol{t}_{\text{stoa}} > \boldsymbol{t}_{\text{toa}}$ or $\boldsymbol{t}_{\text{stoa}} < \boldsymbol{t}_{\text{toa}}$. For those $\boldsymbol{t}_{\text{stoa}}$ with $A(\boldsymbol{t}_{\text{stoa}}) = 0$, $\boldsymbol{t}_{\text{stoa}} \neq \boldsymbol{t}_{\text{toa}}$, $f(\boldsymbol{t}_{\text{stoa}}) > 0$ because at least one $t_{\text{stoa},n}$ is for noise peak, rather than signal peak. ■

Thus, the optimum $\boldsymbol{s}$ can be obtained as follows:

$$\begin{aligned} \boldsymbol{s}_{\text{opt}} &= \underset{\boldsymbol{s_q}}{\text{argmin}}\, g(\boldsymbol{s_q}) \\ \text{s.t. } & \boldsymbol{s_q} \in \boldsymbol{S} \end{aligned} \tag{25}$$

Remark 3: In this research, we set λ_1 and λ_2 to one

C. Extension to Multi User Case

The performance of ToA estimation in the presence of MUI can be degraded. Some techniques such as the successive MUI cancellation estimator [6], [25], are proposed to mitigate the MUI. Since the ToA is estimated by iteratively subtracting MUI from the received signal, these algorithms have error propagation problems. In this paper, we extend our work in the single user case to the multi user case and propose a novel MU-JToAE algorithm which can extract ToA of the desired user by finding the minimum value of the average of $g(\boldsymbol{s_q})$ across different frames without error propagation.

We assume that the TH sequence $\boldsymbol{c_m} = [c_{1,m}\, c_{1,m}\, \cdots\, c_{K,m}]$ for each user is known to the base stations and $\boldsymbol{c_m} \neq \boldsymbol{c_\ell}, m \neq \ell$. A de-spreading process can be performed by each base station, that is, dividing the observation time into *K* equal intervals, each of which is with a period of *T*, $T < T_f$. We define I_k as the *k*-th interval and it can be expressed by $I_k = [c_{k,m} + (k-1) T_f, c_{k,m} + (k-1)T_f + T], m = 1 \cdots M, k = 1 \cdots K$. We assume that the delay spread of the channel is smaller than one frame duration. We denote the correlated signal in the *k*-th interval at the *n*-th base station as $z_{k,n}(t)$ and it can be obtained by posing a window function with duration of I_k to the correlated signal in (5). Then the correlated signal at the *n*-th base station has the *K* waveforms and can be expressed by

$$\begin{aligned} z_{k,n}(t) &= z_n\left(t + (k-1)\, T_f\right) \\ &= R_{S,m}(t) + R_{I,k}(t) + R_{w,k}(t) \end{aligned} \tag{26}$$

where $k = 1 \cdots K$, $0 \leq t \leq T$, $R_{S,m}(t)$ is the desired signal for the *m*-th user, $R_{I,k}(t)$ is the sum of interference from other *M*-1 users. The signal $R_{S,m}(t)$ is the same for all *K* waveforms while $R_{I,k}(t)$ is different for different waveforms because the de-spreading process is performed using the TH sequence for the *m*-th user and thus each waveform has a same starting point, while $R_{I,k}(t)$ has different starting point due to different TH sequence [6].

Let us define $A_{k,m}(\boldsymbol{s_q})$ and $f_{k,m}(\boldsymbol{s_q})$ as the MSSD and MSE function created by $\boldsymbol{s_q}$ for the *k*-th interval and *m*-th user and $g_{k,m}(\boldsymbol{s_q}) = A_{k,m}(\boldsymbol{s_q}) + f_{k,m}(\boldsymbol{s_q})$. Then we have $\sum_{k=1}^{K} g_{k,m} (\boldsymbol{t}_{\text{lec}}) = 0$ because $R_{S,m}(t)$ is the same for all *K* waveforms. If $\boldsymbol{s}_{MPC} \neq \boldsymbol{t}_{\text{toa}}$, where $\boldsymbol{s}_{MPC}$ contains at least one MPC from interferers or one noise peak, then $\frac{1}{K}\sum_{k=1}^{K} g_{k,m}\left(\boldsymbol{t}_{\text{toa}}\right)$ has extremely low possibility being zero due to the fact that $R_{I,k}(t)$ has different peak locations for different *k*. Therefore, the ToA of the first path of the *m*-th user can be determined by

$$\begin{aligned} \boldsymbol{s_{m,\text{opt}}} &= \underset{\boldsymbol{s_q}}{\text{argmin}} \frac{1}{K}\sum_{k=1}^{K} g_{k,m}(\boldsymbol{s_q}) \\ &\text{s.t. } \boldsymbol{s_q} \in \boldsymbol{S} \end{aligned} \tag{27}$$

The equation (27) shows that our approach has no error propagation problem because the base stations can do de-spreading process for each user from 1 to *M* using its TH sequence. Therefore, our approach is applicable to the multi user case with reasonable number of users. For a large amount of users, users can be grouped and localization signals for different groups can be separated in either time or frequency domain.

D. JToAE Algorithm and Its Complexity Analysis

The JToAE algorithm can be found in Algorithm 1. The time consumption of Algorithm 1 mainly originates from calculation of $A(\boldsymbol{s_q})$ and $f(\boldsymbol{s_q})$ for each $\boldsymbol{s_q} \in \boldsymbol{S}$ for the first interval with computational complexity of $O(M\prod_{n=1}^{N} K_n)$ and calculation of $g(\boldsymbol{s_q})$ for the k-th interval with those of $O(MK)$, and thus the total computational complexity of Algorithm 1 is $O(M\prod_{n=1}^{N} K_n + MK)$.

Algorithm 1: JToAE algorithm.

Parameters: M: the number of users, K: the number of frames, $\boldsymbol{c}_m$: TH sequence for the m-th user, K_n: the number of correlation peaks for the n-th received signal
for $m = 1{:}M$ **do**
  Obtain K intervals at each received signal using $\boldsymbol{c}_m$
  $\boldsymbol{G_k} = []$, $k = 1,2,...,K$; $\boldsymbol{U} = []$
  for $k = 1{:}K$ **do**
   if the first interval **then**
    Determine K_n correlation peaks via (8), establish the search space $\boldsymbol{S}$
    for each element $\boldsymbol{s_q}$ in $\boldsymbol{S}$ **do**
     calculate $A(\boldsymbol{s_q})$ via (9), $f(\boldsymbol{s_q})$ via (10), (11) and (12) using the signal in the first interval; $g(\boldsymbol{s_q}) = A(\boldsymbol{s_q}) + f(\boldsymbol{s_q})$; $\boldsymbol{U} = [\boldsymbol{U}\, \boldsymbol{s_q}]$; $\boldsymbol{G_k} = [\boldsymbol{G_k}\; g(\boldsymbol{s_q})]$
    end
   else
    calculate $g(\boldsymbol{s_q})$ using the signal in the k-th interval; $\boldsymbol{G_k} = [\boldsymbol{G_k}\; g(\boldsymbol{s_q})]$
   end
  end
   averaging over K intervals: $\boldsymbol{G} = \frac{\mathbf{1}}{\boldsymbol{K}}\sum_{\boldsymbol{k=1}}^{\boldsymbol{K}} \boldsymbol{G_k}$; $\boldsymbol{s_{m,\text{opt}}} = \text{argmin}_{\boldsymbol{s_q} \in \boldsymbol{S}} \boldsymbol{G}$
end

To further reduce computational complexity, we add the codes that firstly check if two circles can intersect at a point. If any of two peaks in $\boldsymbol{s_q}$ are unable to create intersection, the inner loop will be skipped. Note that computational complexity becomes very high when the number of receivers goes large. To reduce the complexity with large number of receivers, we classify the receivers into $\lfloor N/L \rfloor$ groups, each of which is with L receivers. The MSSD $A(\boldsymbol{s_q})$ and MSE function $f(\boldsymbol{s_q})$ are calculated for each element of search space for each group, and thus the total computational complexity becomes $O(M\sum_{1}^{\lfloor N/L \rfloor}\prod_{n=1}^{L} K_n + MK)$. The selection of L should guarantee that rank of $\boldsymbol{H_q}$ in (9) is no less than three and four for two-dimensional and three-dimensional cases, respectively.

V. Results and Discussion

In this section, we provide some numerical results to show the effectiveness of the proposed JToAE and compare to some other existing methods in terms of RMSE (Root Mean Squared Error) of estimated ToA for each user, which is obtained by 5000-loop Monte-Carlo simulation. We also compare the computational complexity of JToAE to those of the successive MUI cancellation techniques for different number of users.

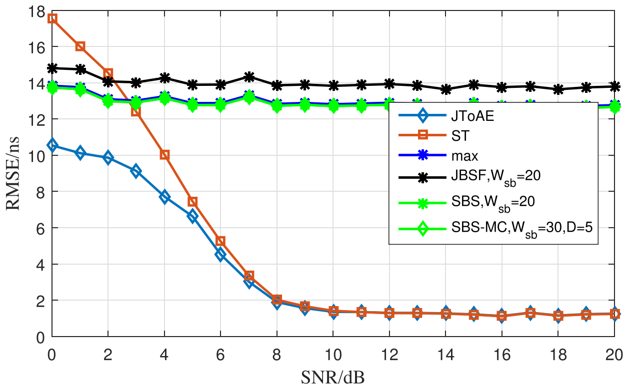

Fig. 1. RMSE for ST, Max, JBSF, SBS, SBS-MC and proposed JToAE with IEEE 802.15.4a channel models: CM3 as a function of SNR. The signal is Time Hopping with $T_f = 128$ ns.The pulse duration $T_c = 2$ ns, and the symbol duration is 512 ns. The bandpass pulse has second derivative Gaussian shape. The signal bandwidth $B = 2.65$ GHz. $N = 3$, $M = 1$.

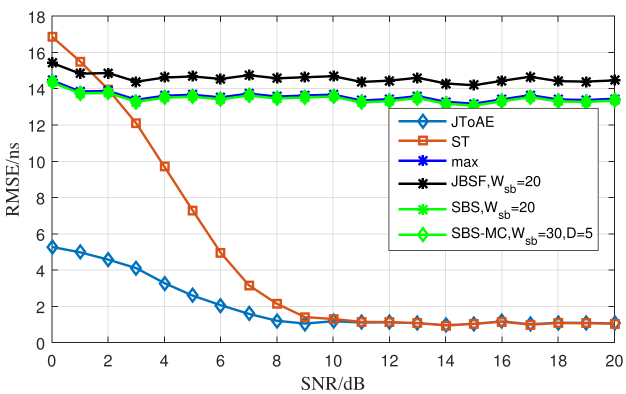

Fig. 2. RMSE for ST, Max, JBSF, SBS, SBS-MC and proposed JToAE with IEEE 802.15.4a channel models: CM1 as a function of SNR. The signal is Time Hopping with $T_f = 128$ ns.The pulse duration $T_c = 2$ ns, and the symbol duration is 512 ns. The bandpass pulse has second derivative Gaussian shape. The signal bandwidth $B = 2.65$ GHz. $N = 3$, $M = 1$.

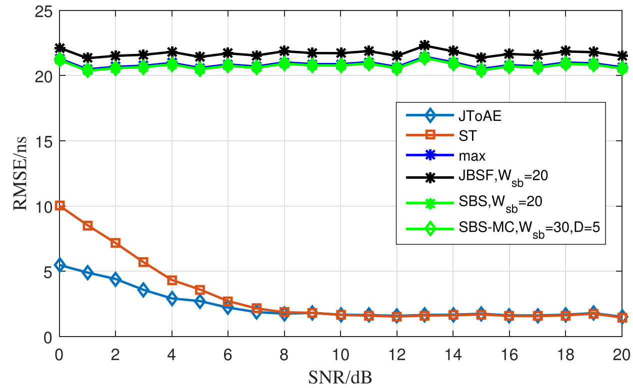

Fig. 3. RMSE for ST, Max, JBSF, SBS, SBS-MC and proposed JToAE with IEEE 802.15.4a channel models: CM5 as a function of SNR. The signal is Time Hopping with $T_f = 128$ ns.The pulse duration $T_c = 2$ ns, and the symbol duration is 512 ns. The bandpass pulse has second derivative Gaussian shape. The signal bandwidth $B = 2.65$ GHz. $N = 3$, $M = 1$.

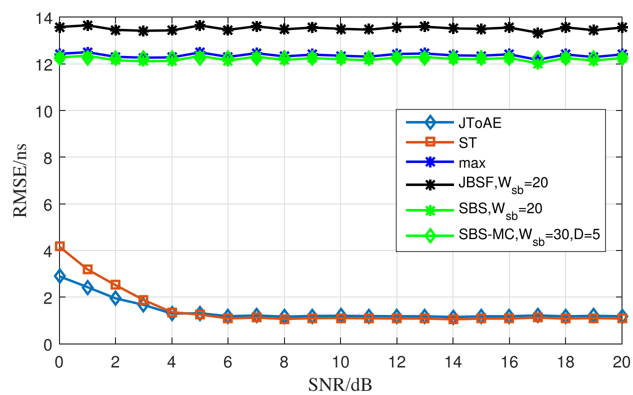

Fig. 4. RMSE for ST, Max, JBSF, SBS, SBS-MC and proposed JToAE with IEEE 802.15.4a channel models: CM7 as a function of SNR. The signal is Time Hopping with $T_f = 128$ ns.The pulse duration $T_c = 2$ ns, and the symbol duration is 512 ns. The bandpass pulse has second derivative Gaussian shape. The signal bandwidth $B = 2.65$ GHz. $N = 3$, $M = 1$.

The performance are evaluated considering UWB IR (Impulse Radio) with second derivative of Gaussian mono-cycle. We consider the chip duration $T_{\mathrm{c}} = 2$ ns, the frame duration $T_f = 128$ ns, the pulse duration $T_{\mathrm{p}} = 2$ ns, the number of chips within one frame $N_{\mathrm{c}} = 64$ and the investigated number of frames are $N_f = 4$, which is compliant with IEEE 802.15.4a [27]. Each element of the TH sequence is randomly generated between 1 and N_{c}. All results are obtained through simulations considering IEEE 802.15.4a channel models CM1 (residential LoS), CM3 (office LoS), CM5 (outdoor LoS) and CM7 (industrial LoS). These channel models assume that the ray arrives in clusters with a rate of Possion distribution $\Lambda_{\mathrm{cm1}} = 0.047\,\mathrm{ns}^{-1}$, $\Lambda_{\mathrm{cm3}} = 0.016\,\mathrm{ns}^{-1}$, $\Lambda_{\mathrm{cm5}} = 0.0448\,\mathrm{ns}^{-1}$ and $\Lambda_{\mathrm{cm7}} = 0.0709\,\mathrm{ns}^{-1}$. The channel realizations are sampled with the rate of 8 GHz, and 3000 different realizations are generated.

We compare to other six methods: Max [28], Simple Thresholding (ST) [29], Jump Back and Search Forward (JBSF) [23], Serial Backward Search (SBS) [23], Serial Backward Search for Multiple Clusters (SBS-MC) [30] and iterative successive MUI cancellation technique [6], [25]. The Max approach aims to select the sample with maximum energy as estimate of the ToA; the ST method is to compare each energy sample to a fixed threshold within a certain observation interval, and take the first threshold crossing sample as the ToA estimate. The threshold for ST can be obtained by (6), that is $\xi = \frac{|v_{n,\max}|}{\sqrt{\eta}}$, where $v_{n,\max}$ is the amplitude of the strongest peak and η is the relative threshold and is set to be 17.23; JBSF approach is based on the detection of the strongest sample and a forward search procedure; SBS method is based on the detection of the strongest sample and a search-back procedure and SBS-MC is to continue the backward search until more than D consecutive noise samples are encountered [12]. The iterative successive MUI cancellation technique utilizes successive cancellation of users with maximum received energy where ToA of each user is iteratively estimated via finding the maximum value from the residual signal.

Fig. 1–4 illustrate the performance of JToAE and make comparisons with other five existing methods for IEEE 802.15.4a CM3, CM1, CM5 and CM7 channel model, respectively. The vertical axis represents the root mean squared error (RMSE) in nanosecond while the horizontal axis gives SNR over $0 \sim 20$ dB. It can be seen that our proposed method dominantly outperforms Max, JBSF, SBS and SBS-MC in the whole SNR region and ST method in the low SNR region of $0 \sim 10$dB for CM3 and CM1 channel. For CM5 and CM7 channel, JToAE shows an evident

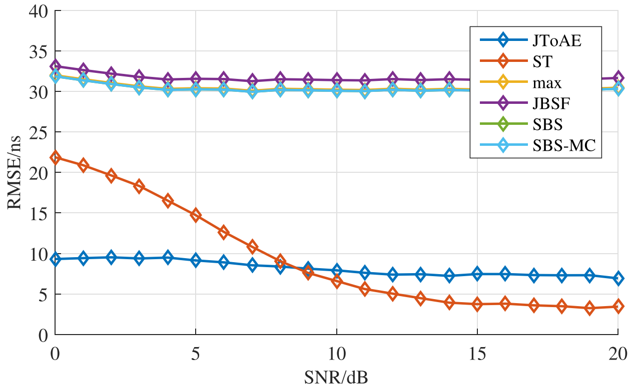

Fig. 5. RMSE for ST, Max, JBSF, SBS, SBS-MC and proposed JToAE with IEEE 802.15.4a channel models: CM1 as a function of SNR. The signal is Time Hopping with $T_f = 128$ ns.The pulse duration $T_c = 2$ ns, and the symbol duration is 512 ns. The bandpass pulse has second derivative Gaussian shape. The signal bandwidth $B = 2.65$ GHz. $N = 3$, $M = 2$.

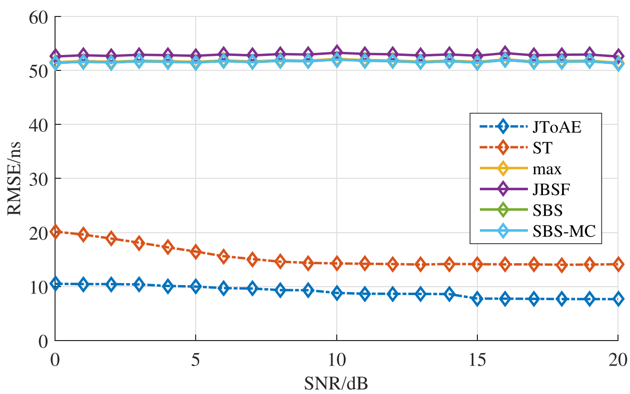

Fig. 6. RMSE for ST, Max, JBSF, SBS, SBS-MC and proposed JToAE with IEEE 802.15.4a channel models: CM1 as a function of SNR. The signal is Time Hopping with $T_f = 128$ ns.The pulse duration $T_c = 2$ ns, and the symbol duration is 512 ns. The bandpass pulse has second derivative Gaussian shape. The signal bandwidth $B = 2.65$ GHz. $N = 3$, $M = 3$.

superiority over Max, JBSF, SBS and SBS-MC in the whole SNR region and moderately outperforms ST method in the low SNR region. It is known that CM1 and CM3 channel models have larger MPC decay than CM5 and CM7. The dominant superiority over other five methods presents in CM1 and CM3 channel models.

Fig. 5–8 compare the RMSE of JToAE to those of the five exiting methods for $M = 1, 2, \ldots, 5$, respectively. Through comparison, we can see that the performance of Max, JBSF, SBS and SBS-MC degrade quickly with increase of number of users while JToAE shows no dominant performance degradation because of its robustness against MUI. ST method outperforms other four existing methods but is inferior than JToAE except in the high SNR region $[10\,\text{dB}, 20\,\text{dB}]$ for $M = 2$ case, JToAE does not depict superiority over ST. With increase of MUI, JToAE dominantly outperforms other five existing methods.

Fig. 9 compares the RMSE with the proposed scheme and the successive MUI cancellation technique as a function of SNR. Notice that the gap between the proposed scheme and the successive MUI cancellation technique is approximately 20 ns in the noise dominated regime. With increase of SNR, signal to

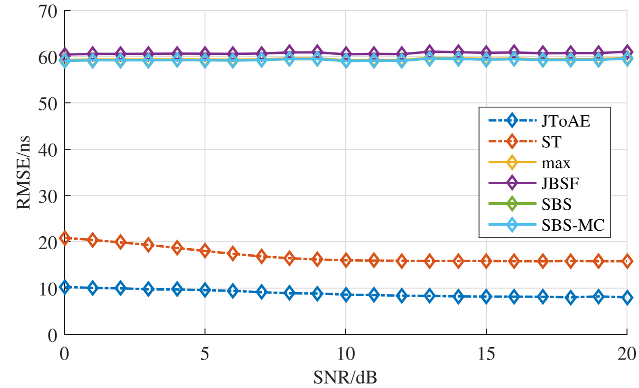

Fig. 7. RMSE for ST, Max, JBSF, SBS, SBS-MC and proposed JToAE with IEEE 802.15.4a channel models: CM1 as a function of SNR. The signal is Time Hopping with $T_f = 128$ ns.The pulse duration $T_c = 2$ ns, and the symbol duration is 512 ns. The bandpass pulse has second derivative Gaussian shape. The signal bandwidth $B = 2.65$ GHz. $N = 3$, $M = 4$.

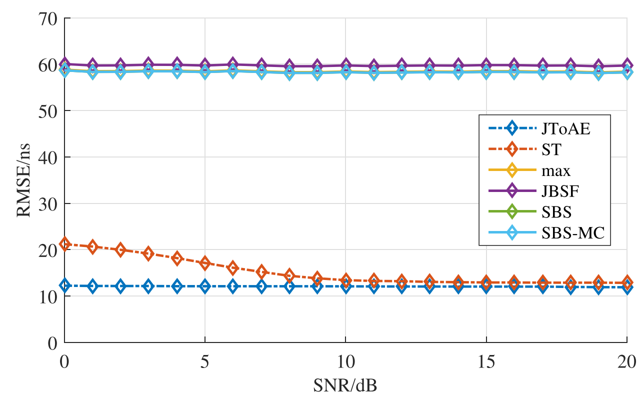

Fig. 8. RMSE for ST, Max, JBSF, SBS, SBS-MC and proposed JToAE with IEEE 802.15.4a channel models: CM1 as a function of SNR. The signal is Time Hopping with $T_f = 128$ ns.The pulse duration $T_c = 2$ ns, and the symbol duration is 512 ns. The bandpass pulse has second derivative Gaussian shape. The signal bandwidth $B = 2.65$ GHz. $N = 3$, $M = 5$.

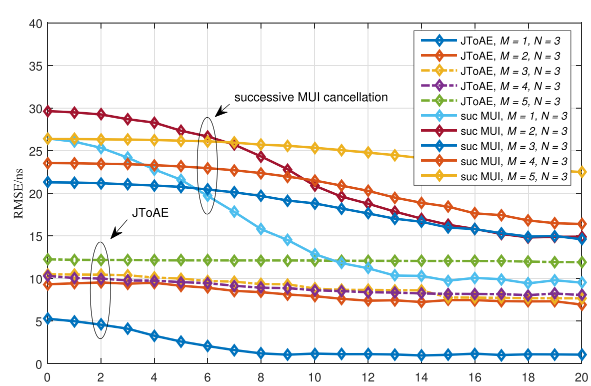

Fig. 9. RMSE for proposed JToAE and iterative successive interference cancellation technique with CM1 as a function of SNR for $M = 1,2,\ldots,5$ and $N = 3$. The signal is Time Hopping with $T_f = 128$ ns.The pulse duration $T_c = 2$ ns, and the symbol duration is 512 ns. The bandpass pulse has second derivative Gaussian shape. The signal bandwidth $B = 2.65$ GHz.

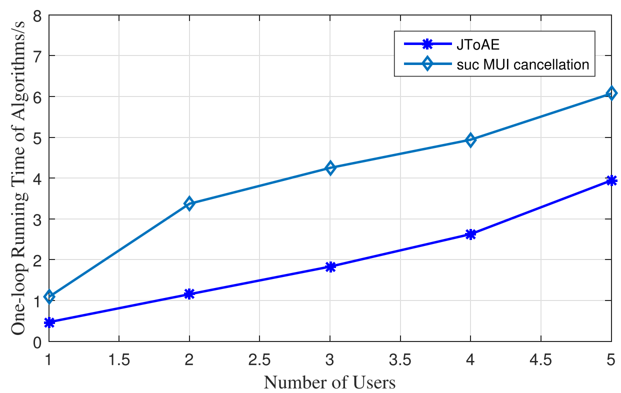

Fig. 10. One-loop running time of JToAE and successive MUI cancellation algorithm for $M = 1,2,...,5$, $N = 3$.

interference ratio (SIR) becomes a dominant factor influencing the performance and the gap between two schemes becomes smaller. It indicates that the proposed scheme has strong robustness against noise. When the SNR increases but SIR keeps constant, the performance improvement becomes slower than the successive MUI cancellation technique.

Fig. 10 compares the computational complexity in terms of one-loop running time of JToAE and successive MUI cancellation techniques for different number of users. We can see that the running time of both algorithms increases approximately linearly with the number of users and the running time of JToAE is dominantly lower than that of successive MUI cancellation technique.

VI. Conclusions

This paper proposed a high accuracy joint ToA estimation scheme which detects the ToA of UWB received signal by fully exploring the spatial information of each base station and incorporating the MSE function introduced by a low-complexity one-pulse ML estimator, which simplify the estimation process via posing a window function to the received signal and thus does not require the knowledge about the number of channels. We firstly described how to utilize spatial information of base stations and the captured correlation peaks to determine MSSD without having to achieve synchronization between transmitters and receivers. Then we proved that sum of MSSD and the MSE function introduced by the one-pulse ML estimator has a unique global minimum at the actual ToA vector. We showed that our proposed scheme can be easily extended to the multi user case.

To verify the effectiveness of our scheme, we performed Monto-Carlo simulation using IEEE 802.15.4a channel models and compared the simulation results to those created by other existing methods: ST, Max, JBSF, SBS, SBS-MC and successive MUI cancellation. The results show that our scheme achieves a dominant superiority over the existing methods in terms of robustness against MUI and multipath transmission.

Appendix A
Proof of Lemma 1

In this section, we give the proof of Lemma 1. The denominator of LHS (Left Hand Side) and RHS (Right Hand Side) of (20) can be approximated as

$$\int_{-T_{\mathrm{p}}/2}^{T_{\mathrm{p}}/2} p^2\left(t-\hat{\tau}_n\right) \mathrm{d}t \approx E_{\mathrm{p}}$$

$$\int_{-T_{\mathrm{p}}/2}^{T_{\mathrm{p}}/2} p\left(t-\hat{\tau}_n\right) p'\left(t-\hat{\tau}_n\right) \mathrm{d}t = \frac{1}{2} p^2\left(T_{\mathrm{p}}/2-\left|\hat{\tau}_n\right|\right) \quad (28)$$

where E_{p} is pulse energy. The nominator of LHS and RHS of (20) can be further derived as

$$\int_{-T_{\mathrm{p}}/2}^{T_p/2} w_n(t) p\left(t-\hat{\tau}_n\right) \mathrm{d}t = R_{pw}(\hat{\tau}_n)$$

$$\int_{-T_{\mathrm{p}}/2+\sigma}^{T_p/2} p\left(t-\sigma_n\right) p\left(t-\hat{\tau}_n\right) \mathrm{d}t = R_p\left(\hat{\tau}_n-\sigma_n\right)$$

$$\int_{-T_{\mathrm{p}}/2}^{T_p/2} w_n(t) p'\left(t-\hat{\tau}_n\right) \mathrm{d}t = R_{p'w}(\hat{\tau}_n)$$

$$\int_{-T_p/2+\sigma}^{T_p/2} p\left(t-\sigma_n\right) p'\left(t-\hat{\tau}_n\right) \mathrm{d}t = R_{pp'}\left(\hat{\tau}_n-\sigma_n\right) \quad (29)$$

Thus, (20) can be approximated as

$$\frac{R_{pw}(\hat{\tau}_n)+a_n R_p\left(\hat{\tau}_n-\sigma_n\right)}{E_{\mathrm{p}}} \approx \frac{R_{p'w}(\hat{\tau}_n)+a_n R_{pp'}\left(\hat{\tau}_n-\sigma_n\right)}{p^2\left(T_{\mathrm{p}}/2-\left|\hat{\tau}_n\right|\right)/2} \quad (30)$$

From (21), the optimum $\hat{a}_n$ can be approximated as

$$\hat{a}_n \approx \frac{R_{pw}(\hat{\tau}_n)+a_n R_p\left(\hat{\tau}_n-\sigma_n\right)}{E_{\mathrm{p}}} \quad (31)$$

To find a closed expression of $\hat{\tau}_n$ and $\hat{a}_n$, (30) should be transformed to

$$2a_n E_p R_{pp'}\left(\hat{\tau}_n-\sigma_n\right) - a_n p^2\left(T_{\mathrm{p}}/2-\left|\hat{\tau}_n\right|\right) R_p\left(\hat{\tau}_n-\sigma_n\right) \approx p^2\left(T_{\mathrm{p}}/2-\left|\hat{\tau}_n\right|\right) R_{pw}(\hat{\tau}_n) - 2E_p R_{p'w}(\hat{\tau}_n) \quad (32)$$

Then (32) can be further simplified as

$$R_{p,E_p p'-\gamma p}\left(\hat{\tau}_n-\sigma_n\right) \approx \frac{\beta}{a_n} \quad (33)$$

where $\gamma = \frac{1}{2}p^2(T_{\mathrm{p}}/2-|\hat{\tau}_n|)$, $R_{p,E_p p'-\gamma p}(\tau) = \int_{-T_p/2}^{T_p/2} p(t)$ $(E_{\mathrm{p}}p'(t-\tau)-\gamma p(t-\tau))\mathrm{d}t$, $\beta = \gamma R_{pw}(\hat{\tau}_n) - E_p R_{p'w}(\hat{\tau}_n)$ and can be considered as a Gaussian variable. From (33), the optimum $\hat{\tau}_n$ can be approximated by

$$\hat{\tau}_n \approx \sigma_n + R^{-1}_{p,E_p p'-\gamma p}\left(\frac{\beta}{a_n}\right) \quad (34)$$

Recall that the normalized UWB pulse is employed in our paper. Hence, $E_{\mathrm{p}} = 1$ and thus (34) and (31) can be simplified as

$$\hat{\tau}_n \approx \sigma_n + R^{-1}_{p,p'-\gamma p}\left(\frac{\beta}{a_n}\right)$$

$$\hat{a}_n = R_{pw}(\hat{\tau}_n) + a_n R_p\left(\hat{\tau}_n-\sigma_n\right) = R_{pw}(\hat{\tau}_n) + a_n R_p\left(R^{-1}_{p,p'-\gamma p}\left(\frac{\beta}{a_n}\right)\right) \quad (35)$$

From (35), it is clear that $R^{-1}_{p,p'-\gamma p}(\frac{\beta}{a_n})$ is a random variable depending on $\hat{\tau}_n$ and $w_n(t)$, where $\hat{\tau}_n$ is correlated to $w_n(t)$. Thus, it is a non-trivial issue to give a closed expression for $\hat{\tau}_n$. In what follows, we will firstly derive the expectation and variance of $\hat{\tau}_n$ estimated by the one-pulse ML estimator, and then give the closed expression for $f(\boldsymbol{s_q})$. From [31], we can know that for any objective function $F(\tau)$, which is differential up to the second order, the time delay converges to

$$\hat{\tau}_{\rm b} - \tau_{\rm b} \cong -\frac{\frac{\partial}{\partial \tau}F(\tau)\,|\tau=\tau_{\rm b}}{E_w\left(\frac{\partial^2}{\partial \tau^2}F(\tau)\,|\tau=\tau_{\rm b}\right)} \tag{36}$$

with probability one, where $\hat{\tau}_{\rm b}$ and $\tau_{\rm b}$ are the estimated and real time delay, respectively. Recall that the objective function of the one-pulse MLE is $F(\tilde{\tau}_n, \tilde{a}_n, \sigma_n, a_n)$, where $\tilde{\tau}_n$ and $\tilde{a}_n$ are the searched time delay and amplitude, respectively, and $\sigma_n = t_{q,n} - \hat{t}_{q,n}$. From (16), the first derivative of $F(\tilde{\tau}_n, \tilde{a}_n, \sigma_n, a_n)$ at the real time delay $\tilde{\tau}_n = \sigma_n$ can be determined by

$$\frac{\partial F(\tilde{\tau}_n, \tilde{a}_n, \sigma_n, a_n)}{\partial \tilde{\tau}_n}|_{\tilde{\tau}_n=\sigma_n} = 2\tilde{a}_n \begin{bmatrix} \int_{-T_{\rm p}/2}^{T_{\rm p}/2} w_n(t)p'(t-\sigma_n)\,{\rm d}t \\ -\tilde{a}_n\int_{-T_{\rm p}/2}^{T_{\rm p}/2} p(t-\sigma_n)\,p'(t-\sigma_n)\,{\rm d}t \\ +a_n\int_{-T_{\rm p}/2+\sigma_n}^{T_{\rm p}/2} p(t-\sigma_n)\,p'(t-\sigma_n)\,{\rm d}t \end{bmatrix}$$

and its second derivative can be determined by

$$\frac{\partial^2 F(\tilde{\tau}_n, \tilde{a}_n, \sigma_n, a_n)}{\partial \tilde{\tau}_n^2}|_{\tilde{\tau}_n=\sigma_n} = 2\tilde{a}_n \begin{bmatrix} -\int_{-T_{\rm p}/2}^{T_{\rm p}/2} w_n(t)p'(t-\sigma_n)\,{\rm d}t \\ +\tilde{a}_n\int_{-T_{\rm p}/2}^{T_{\rm p}/2} p'^2(t-\sigma_n)\,{\rm d}t \\ +\tilde{a}_n\int_{-T_{\rm p}/2}^{T_{\rm p}/2} p(t-\sigma_n)\,p''(t-\sigma_n)\,{\rm d}t \\ -a_n\int_{-T_{\rm p}/2+\sigma_n}^{T_{\rm p}/2} p(t-\sigma_n)\,p''(t-\sigma_n)\,{\rm d}t \end{bmatrix}$$

From (36), the estimated time delay converges almost surely to

$$\hat{\tau}_n \cong -\frac{\begin{bmatrix} R_{p'w}(\sigma_n) + \frac{a_n}{2}p^2\left(\frac{T_{\rm p}}{2}-\sigma_n\right) - \\ \frac{\hat{a}_n}{2}\left(p^2\left(\frac{T_{\rm p}}{2}-\sigma_n\right) - p^2\left(-\frac{T_{\rm p}}{2}-\sigma_n\right)\right) \end{bmatrix}}{E\begin{bmatrix} -R_{p'w}(\sigma_n) \\ +(\hat{a}_n - a_n)\,p\left(\frac{T_{\rm p}}{2}-\sigma_n\right)p'\left(\frac{T_{\rm p}}{2}-\sigma_n\right) \\ -\hat{a}_n p\left(\frac{T_{\rm p}}{2}+\sigma_n\right)p'\left(\frac{T_{\rm p}}{2}+\sigma_n\right) \\ +a_n\int_{-T_{\rm p}/2+\sigma_n}^{T_{\rm p}/2} p'^2(t-\sigma_n)\,{\rm d}t \end{bmatrix}} \tag{37}$$

Substituting $\hat{a}_n$ with $R_{pw}(\hat{\tau}_n) + a_n R_p(\hat{\tau}_n - \sigma_n)$ given by (35), Lemma 1 can be proved.

Appendix B
Proof of Lemma 2

We transform (22) to

$$\hat{\tau}_n \begin{bmatrix} (a_n R_p(\hat{\tau}_n - \sigma_n) - a_n) \\ \times p\left(\frac{T_{\rm p}}{2}-\sigma_n\right)p'\left(\frac{T_{\rm p}}{2}-\sigma_n\right) \\ -a_n R_p(\hat{\tau}_n - \sigma_n) \\ \times p\left(\frac{T_{\rm p}}{2}+\sigma_n\right)p'\left(\frac{T_{\rm p}}{2}+\sigma_n\right) \\ +a_n\int_{-T_{\rm p}/2+\sigma_n}^{T_{\rm p}/2} p'^2(t-\sigma_n)\,{\rm d}t \end{bmatrix}$$

$$= -\begin{bmatrix} R_{p'w}(\sigma_n) + \frac{a_n}{2}p^2\left(\frac{T_{\rm p}}{2}-\sigma_n\right) - \\ \frac{R_{pw}(\hat{\tau}_n)+a_nR_p(\hat{\tau}_n-\sigma_n)}{2}\begin{bmatrix} p^2\left(\frac{T_{\rm p}}{2}-\sigma_n\right) - \\ p^2\left(-\frac{T_{\rm p}}{2}-\sigma_n\right) \end{bmatrix} \end{bmatrix} \tag{38}$$

By using first-order Taylor expansion around $\hat{\tau}_n = \sigma_n$ for LHS and RHS of (38), we can obtain

$$\begin{bmatrix} a_n\sigma_n p\left(\frac{T_{\rm p}}{2}-\sigma_n\right)p'\left(\frac{T_{\rm p}}{2}-\sigma_n\right) \\ +a_n\left(1+\sigma_n R_{\rm p}'(0)\right) \\ \times p\left(\frac{T_{\rm p}}{2}-\sigma_n\right)p'\left(\frac{T_{\rm p}}{2}-\sigma_n\right)E(\hat{\tau}_n) \\ -a_n p\left(\frac{T_{\rm p}}{2}-\sigma_n\right)p'\left(\frac{T_{\rm p}}{2}-\sigma_n\right)E(\hat{\tau}_n) \\ -a_n\left(\sigma_n + \left(1+\sigma_n R_{\rm p}'(0)\right)E(\hat{\tau}_n)\right) \\ \times p\left(\frac{T_{\rm p}}{2}+\sigma_n\right)p'\left(\frac{T_{\rm p}}{2}+\sigma_n\right) \\ +a_n E(\hat{\tau}_n)\int_{-T_{\rm p}/2+\sigma_n}^{T_{\rm p}/2} p'^2(t-\sigma_n)\,{\rm d}t \end{bmatrix}$$

$$\approx \begin{bmatrix} -\frac{a_n}{2}p^2\left(\frac{T_{\rm p}}{2}-\sigma_n\right) \\ +\frac{a_n}{2}\left(p^2\left(\frac{T_{\rm p}}{2}-\sigma_n\right) - p^2\left(-\frac{T_{\rm p}}{2}-\sigma_n\right)\right) \\ +\frac{a_n}{2}R_{\rm p}'(0)\,E(\hat{\tau}_n) \\ \times\left(p^2\left(\frac{T_{\rm p}}{2}-\sigma_n\right) - p^2\left(-\frac{T_{\rm p}}{2}-\sigma_n\right)\right) \end{bmatrix} \tag{39}$$

Thus, the expectation and variance of $\hat{\tau}_n$ can be approximated by

$$E(\hat{\tau}_n) \approx \frac{\begin{matrix} -\frac{1}{2}p^2\left(-\frac{T_{\rm p}}{2}-\sigma_n\right) \\ -\sigma_n p\left(\frac{T_{\rm p}}{2}-\sigma_n\right)p'\left(\frac{T_{\rm p}}{2}-\sigma_n\right) \\ +\sigma_n p\left(\frac{T_{\rm p}}{2}+\sigma_n\right)p'\left(\frac{T_{\rm p}}{2}+\sigma_n\right) \end{matrix}}{\begin{matrix} \int_{-T_{\rm p}/2+\sigma_n}^{T_{\rm p}/2} p'^2(t-\sigma_n)\,{\rm d}t \\ -p\left(\frac{T_{\rm p}}{2}+\sigma_n\right)p'\left(\frac{T_{\rm p}}{2}+\sigma_n\right) \end{matrix}} \tag{40}$$

and

$$var(\hat{\tau}_n) \approx \frac{\left[\begin{array}{c}\int_{-T_p/2-\sigma_n}^{T_p/2} p'^2(t)\mathrm{d}t+\\ \frac{1}{4}\left[p^2\left(\frac{T_p}{2}-\sigma_n\right)-p^2\left(-\frac{T_p}{2}-\sigma_n\right)\right]^2\end{array}\right]\sigma_N^2}{\left[\begin{array}{c}a_n\int_{-T_p/2+\sigma_n}^{T_p/2} p'^2(t-\sigma_n)\mathrm{d}t\\ -a_n p\left(\frac{T_p}{2}-\sigma_n\right)p'\left(\frac{T_p}{2}-\sigma_n\right)\end{array}\right]^2} \tag{41}$$

when $\sigma_n = 0$, (40) and (41) can be simplified as

$$E(\hat{\tau}_n) = 0; var(\hat{\tau}_n) = \frac{\sigma_N^2}{4\pi^2 a_n^2 \int_{-B/2}^{B/2} f^2 |P(f)|^2 \mathrm{d}f} \tag{42}$$

Then Lemma 2 is proved.

Appendix C
Proof of Theorem 1

By replacing $\tilde{\tau}_n$ and $\tilde{a}_n$ in $F(\tilde{\tau}_n, \tilde{a}_n, \sigma, a_n)$ by the optimum $\hat{\tau}_n$ and $\hat{a}_n$ from (35) , (12) can be rewritten as

$$f(\boldsymbol{s_q}) = \sum_{n=1}^{3} E\left\{\begin{array}{l}\int_{-T_p/2}^{-T_p/2+\sigma_n}\left[\begin{array}{c}w_n(t)\\ -\hat{a}_n p(t-\hat{\tau}_n)\end{array}\right]^2\mathrm{d}t\\ +\int_{-T_p/2+\sigma_n}^{T_p/2}\left[\begin{array}{c}a_n p(t-\sigma_n)\\ -\hat{a}_n p(t-\hat{\tau}_n)\\ +w_n(t)\end{array}\right]^2\mathrm{d}t\end{array}\right\}$$
$$= \sum_{n=1}^{3}\left[\begin{array}{l}T_p + [T_p - E(\hat{\tau}_n)]\left[\int_{-T_p/2}^{T_p/2} p^2(t-E(\hat{\tau}_n))\,\mathrm{d}t - 2\right]\sigma_N^2\\ +a_n^2 R_p^2(E(\hat{\tau}_n)-\sigma_n)\int_{-T_p/2}^{T_p/2} p^2(t-E(\hat{\tau}_n))\,\mathrm{d}t\\ +a_n^2\int_{-T_p/2+\sigma_n}^{T_p/2} p^2(t-\sigma_n)\,\mathrm{d}t - 2a_n^2 R_p^2(E(\hat{\tau}_n)-\sigma_n)\end{array}\right] \tag{43}$$

Then the first derivative of $f(\boldsymbol{s_q})$ with respect to σ_n can be expressed by

$$\frac{\partial f(\boldsymbol{s_q})}{\partial \sigma_n}$$
$$= \sum_{n=1}^{3}\left(\begin{array}{c}-2a_n E\left[\begin{array}{c}R_{pw}(\hat{\tau}_n)R_p'(\hat{\tau}_n-\sigma_n)\\ \times\int_{-T_p/2}^{T_p/2} p^2(t-\hat{\tau}_n)\,\mathrm{d}t\end{array}\right]\\ -2a_n^2 E\left[\begin{array}{c}R_p(\hat{\tau}_n-\sigma_n)R_p'(\hat{\tau}_n-\sigma_n)\\ \times\int_{-T_p/2}^{T_p/2} p^2(t-\hat{\tau}_n)\,\mathrm{d}t\end{array}\right]\\ +2a_n E\left[R_p'(\hat{\tau}_n-\sigma_n)R_{pw}(\hat{\tau}_n)\right]-\\ 2a_n^2\int_{-T_p/2+\sigma_n}^{T_p/2} p(t-\sigma_n)p'(t-\sigma_n)\,\mathrm{d}t\\ +2a_n E\left[\begin{array}{c}R_{pw}(\hat{\tau}_n)R_p'(\hat{\tau}_n-\sigma_n)\\ +2a_n R_p(\hat{\tau}_n-\sigma_n)R_p'(\hat{\tau}_n-\sigma_n)\end{array}\right]\end{array}\right)$$
$$\cong \sum_{n=1}^{3}\left[\begin{array}{c}-2a_n^2 E\left[\begin{array}{c}R_p(\hat{\tau}_n-\sigma_n)R_p'(\hat{\tau}_n-\sigma_n)\\ \times\int_{-T_p/2}^{T_p/2} p^2(t-\hat{\tau}_n)\,\mathrm{d}t\end{array}\right]\\ -2a_n^2\int_{-T_p/2+\sigma_n}^{T_p/2} p(t-\sigma_n)p'(t-\sigma_n)\,\mathrm{d}t\\ +4a_n^2 E\left(R_p(\hat{\tau}_n-\sigma_n)R_p'(\hat{\tau}_n-\sigma_n)\right)\end{array}\right] \tag{44}$$

Note that we use "$\cong$" in (44) as $E_w(R_{pw}(\hat{\tau}_n)R_p'(\hat{\tau}_n-\sigma_n))$ and $E_w\left(\begin{smallmatrix}R_{pw}(\hat{\tau}_n)R_p'(\hat{\tau}_n-\sigma_n)\\ \times\int_{-T_p/2}^{T_p/2} p^2(t-\hat{\tau}_n)\mathrm{d}t\end{smallmatrix}\right)$ almost surely converge to zero. Then the first-order derivative of $f(\boldsymbol{s_q})$ evaluated at $\sigma_n = 0$ can be obtained by

$$\frac{\partial f(\boldsymbol{s_q})}{\partial \sigma_n}\Big|_{\sigma_n=0} \cong \sum_{n=1}^{3}\left(\begin{array}{c}-2a_n^2 E_w\left(R_p(\hat{\tau}_n)R_p'(\hat{\tau}_n)\right)\\ \times\int_{-T_p/2}^{T_p/2} p^2(t-\hat{\tau}_n)\,\mathrm{d}t\\ +4a_n^2 E_w\left(R_p(\hat{\tau}_n)R_p'(\hat{\tau}_n)\right)\end{array}\right) \tag{45}$$

From (43), $\hat{\tau}_n$ can be modeled as a zero mean Gaussian variable. Hence, $E_w(R_p(\hat{\tau}_n)R_p'(\hat{\tau}_n))$ can be derived as

$$E_w\left(R_p(\hat{\tau}_n)R_p'(\hat{\tau}_n)\right) = \frac{\int_{-T_p/2}^{T_p/2} R_p(\hat{\tau}_n)R_p'(\hat{\tau}_n)e^{-\frac{\hat{\tau}_n^2}{2var(\hat{\tau}_n)}}\mathrm{d}\hat{\tau}_n}{\sqrt{2\pi var(\hat{\tau}_n)}} \tag{46}$$

Prior to going further, we firstly show that the *K*-th derivative of $R_p(\tau)$ evaluated at $\tau = 0$ is equal to zero if *K* is odd and $p(t)$ has a symmetric pulse shape. The *K*-th derivative of $R_p(\tau)$ is represented as $R_p^{(K)}(\tau)$ and it can be expressed by

$$R_p^{(K)}(\tau)\,|_{\tau=0} = \sum_{k=0}^{\lfloor K/2\rfloor-1}(-1)^k p^{(k)}(t)p^{(K-1-k)}(t)\Big|_{-T_p/2}^{T_p/2}$$
$$+\frac{1}{2}(-1)^{\lfloor K/2\rfloor}\left(p^{(\lfloor K/2\rfloor)}(t)\right)^2\Big|_{-T_p/2}^{T_p/2} \tag{47}$$

where $\lfloor\rfloor$ denotes floor function. Because *K* is odd and $p(t)$ has a symmetric pulse shape, (46) should be zero. Expanding (45) around $\hat{\tau}_n = 0$ via Taylor series, we can obtain

$$E_w\left(R_p(\hat{\tau}_n)R_p'(\hat{\tau}_n)\right) =$$
$$\int_{-T_p/2}^{T_p/2}\left(\begin{array}{c}R_p(0)R_p'(0)+\\ \sum_{k=1}^{\infty}\frac{1}{k!}\left[\begin{array}{c}R_p(\hat{\tau}_n)\times\\ R_p'(\hat{\tau}_n)\end{array}\right]^{(k)}_{|\hat{\tau}_n=0}\tau_n^k\end{array}\right)e^{-\frac{\hat{\tau}_n^2}{2var(\hat{\tau}_n)}}\mathrm{d}\hat{\tau}_n \tag{48}$$

By the fact that $E(\tau_n^k) = 0$ and $R_p^{(K)}(0) = 0$ if *k* is odd, we can get $E_w(R_p(\hat{\tau}_n)R_p'(\hat{\tau}_n)) = 0$. With a similar way, it can be shown that $E_w(R_p(\hat{\tau}_n)R_p'(\hat{\tau}_n)\int_{-T_p/2}^{T_p/2} p^2(t-\hat{\tau}_n)\mathrm{d}t)$ is also zero. Recall that $f(\boldsymbol{s_q})$ is a mean squared error between the windowed received signal and the estimated one, it can state that $f(\boldsymbol{s_q})$ approaches its local minimum with $\sigma = 0$ and thus Theorem 1 is proved.

References

[1] G. Cheng, "Accurate TOA-based UWB localization system in coal mine based on WSN," *Phys. Procedia*, vol. 24, pp. 534–540, 2012. [Online]. Available: http://www.sciencedirect.com/science/article/pii/S1875389212001216

[2] Z. Sahinoglu, S. Gezici, and I. Guvenc, *Ultra-Wideband Positioning Systems*. Cambridge, U.K.: Cambridge Univ. Press, May 2008. [Online]. Available: http://www.merl.com/publications/TR2008-100

[3] M. Z. Win and R. A. Scholtz, "Characterization of ultra-wide bandwidth wireless indoor channels: A communication-theoretic view," *IEEE J. Sel. Area Commun.*, vol. 20, no. 9, pp. 1613–1627, Sep. 2006, doi: 10.1109/JSAC.2002.805031.

[4] D. Dardari, C. C. Chong, and M. Win, "Threshold-based time-of-arrival estimators in UWB dense multipath channels," *IEEE Trans. Commun.*, vol. 56, no. 8, pp. 1366–1378, Aug. 2008.

[5] D. Dardari, C. C. Chong, and M. Z. Win, "Analysis of threshold-based ToA estimators in UWB channels," in *Proc. 14th Eur. Signal Process. Conf.*, Sep. 2006, pp. 1–6.

[6] V. Kristem, A. F. Molisch, S. Niranjayan, and S. Sangodoyin, "Coherent UWB ranging in the presence of multiuser interference," *IEEE Trans. Wireless Commun.*, vol. 13, no. 8, pp. 4424–4439, Aug. 2014.

[7] H. Ding, W. Liu, X. Huang, and L. Zheng, "First path detection using rank test in IR UWB ranging with energy detection receiver under harsh environments," *IEEE Commun. Lett.*, vol. 17, no. 4, pp. 761–764, Apr. 2013.

[8] A. Giorgetti and M. Chiani, "Time-of-arrival estimation based on information theoretic criteria," *IEEE Trans. Signal Process.*, vol. 61, no. 8, pp. 1869–1879, Apr. 2013.

[9] T. V. Nguyen, Y. Jeong, H. Shin, and M. Z. Win, "Machine learning for wideband localization," *IEEE J. Sel. Areas Commun.*, vol. 33, no. 7, pp. 1357–1380, Jul. 2015.

[10] V. Savic, E. G. Larsson, J. Ferrer-Coll, and P. Stenumgaard, "Kernel methods for accurate UWB-based ranging with reduced complexity," *IEEE Trans. Wireless Commun.*, vol. 15, no. 3, pp. 1783–1793, Mar. 2016.

[11] V. Savic, J. Ferrer-Coll, P.Ängskog, J. Chilo, P. Stenumgaard, and E. G. Larsson, "Measurement analysis and channel modeling for TOA-based ranging in tunnels," *IEEE Trans. Wireless Commun.*, vol. 14, no. 1, pp. 456–467, Jan. 2015.

[12] D. Dardari, A. Conti, U. Ferner, A. Giorgetti, and M. Z. Win, "Ranging with ultrawide bandwidth signals in multipath environments," *Proc. IEEE*, vol. 97, no. 2, pp. 404–426, Feb. 2009.

[13] C. Xu and C. L. Law, "Delay-dependent threshold selection for UWB TOA estimation," *IEEE Commun. Lett.*, vol. 12, no. 5, pp. 380–382, May 2008.

[14] H. Wymeersch, S. Marano, W. M. Gifford, and M. Z. Win, "A machine learning approach to ranging error mitigation for UWB localization," *IEEE Trans. Commun.*, vol. 60, no. 6, pp. 1719–1728, Jun. 2012.

[15] V. Kristem, S. Niranjayan, S. Sangodoyin, and A. F. Molisch, "Experimental determination of UWB ranging errors in an outdoor environment," in *Proc. IEEE Int. Conf. Commun.*, Jun. 2014, pp. 4838–4843.

[16] J.-Y. Lee and R. A. Scholtz, "Ranging in a dense multipath environment using an UWB radio link," *IEEE J. Sel. Areas Commun.*, vol. 20, no. 9, pp. 1677–1683, Dec. 2002.

[17] R. A. Scholtz and J.-Y. Lee, "Problems in modeling UWB channels," in *Proc. Conf. Record 36th Asilomar Conf. Signals, Syst., Comput.*, Nov. 2002, pp. 706–711, vol. 1.

[18] A. A. D'amico, U. Mengali, and L. Taponecco, "Energy-based TOA estimation," *IEEE Trans. Wireless Commun.*, vol. 7, no. 3, pp. 838–847, Mar. 2008.

[19] I. Guvenc and H. Arslan, "Comparison of two searchback schemes for non-coherent TOA estimation in IR-UWB systems," in *Proc. IEEE Sarnoff Symp.*, Mar. 2006, pp. 1–4.

[20] I. Guvenc and Z. Sahinoglu, "Multiscale energy products for TOA estimation in IR-UWB systems," in *Proc. IEEE Global Telecommun. Conf.*, Nov. 2005, vol. 1, pp. 209–213.

[21] D. Dardari, A. Giorgetti, and M. Z. Win, "Time-of-arrival estimation of UWB signals in the presence of narrowband and wideband interference," in *Proc. IEEE Int. Conf. Ultra-Wideband*, Sep. 2007, pp. 71–76.

[22] A. Rabbachin, I. Oppermann, and B. Denis, "Ml time-of-arrival estimation based on low complexity UWB energy detection," in *Proc. IEEE Int. Conf. Ultra-Wideband*, Sep. 2006, pp. 599–604.

[23] I. Guvenc and Z. Sahinoglu, "Threshold-based TOA estimation for impulse radio UWB systems," in *Proc. IEEE Int. Conf. Ultra-Wideband*, Sep. 2005, pp. 420–425.

[24] V. Savic, E. G. Larsson, J. Ferrer-Coll, and P. Stenumgaard, "Kernel principal component analysis for UWB-based ranging," in *Proc. IEEE 15th Int. Workshop Signal Process. Adv. Wireless Commun.*, Jun. 2014, pp. 145–149.

[25] A. G. Amig, A. Mallat, and L. Vandendorpe, "Multiuser and multipath interference mitigation in UWB TOA estimation," in *Proc. IEEE Int. Conf. Ultra-Wideband*, Sep. 2011, pp. 465–469.

[26] M. Flury, R. Merz, and J. Y. L. Boudec, "Synchronization for impulse-radio UWB with energy-detection and multi-user interference: Algorithms and application to IEEE 802.15.4a," *IEEE Trans. Signal Process.*, vol. 59, no. 11, pp. 5458–5472, Nov. 2011.

[27] *IEEE Standard for Information Technology—Telecommunications and Information Exchange Between Systems—Local and Metropolitan Area Networks—Specific Requirement Part 15.4: Wireless Medium Access Control (MAC) and Physical Layer (PHY) Specifications for Low-Rate Wireless Personal Area Networks (WPANs)*, IEEE Standard 802.15.4a-2007 (Amendment to IEEE Standard 802.15.4-2006), pp. 1–203, 2007.

[28] L. Stoica, A. Rabbachin, and I. Oppermann, "A low-complexity noncoherent IR-UWB transceiver architecture with TOA estimation," *IEEE Trans. Microw. Theory Techn.*, vol. 54, no. 4, pp. 1637–1646, Jun. 2006.

[29] D. Dardari, C. C. Chong, and M. Z. Win, "Analysis of threshold-based ToA estimators in UWB channels," in *Proc. 14th Eur. Signal Process. Conf.*, Sep. 2006, pp. 1–6.

[30] I. Guvenc, Z. Sahinoglu, P. Orlik, and H. Arslan, "Searchback algorithms for TOA estimation in non-coherent low-rate IR-UWB systems," *Wireless Pers. Commun.*, vol. 48, no. 4, pp. 585–603, Mar. 2009, doi: 10.1007/s11277-008-9549-3.

[31] B. T. Sieskul, F. Zheng, and T. Kaiser, "A hybrid SS-ToA wireless NLOS geolocation based on path attenuation: Mobile position estimation," in *Proc. IEEE Wireless Commun. Netw. Conf.*, Apr. 2009, pp. 1–6.

Shangbo Wang (S'17–M'18) received the master' s and Dr.-Ing. degrees from the University of Duisburg-Essen, Duisburg, Germany, in 2007 and 2014, respectively. Prior to joining the University of Technology Sydney as a Research Assistant in 2015, he was with Siemens AG, Munich, Germany, as a Research Engineer, and with Continental AG, Lindau, Germany, as a Development Engineer. His research interests include statistical signal processing, intelligent transportation systems, digital signal processing, wireless localization, and mobile communication.

Guoqiang Mao (S'98–M'02–SM'07–F'18) joined the University of Technology Sydney in February 2014 as a Professor of Wireless Networking and the Director of the Center for Real-time Information Networks. Before that, he was with the School of Electrical and Information Engineering, The University of Sydney. He has authored/coauthored more than 200 papers in international conferences and journals, which have been cited more than 7000 times. His research interest includes intelligent transport systems, applied graph theory and its applications in telecommunications, Internet of Things, wireless sensor networks, wireless localization techniques, and network modeling and performance analysis. He has been an editor for the IEEE TRANSACTIONS ON INTELLIGENT TRANSPORTATION SYSTEMS, since 2018, IEEE TRANSACTIONS ON WIRELESS COMMUNICATIONS, since 2014, and IEEE TRANSACTIONS ON VEHICULAR TECHNOLOGY, since 2010. He was the recipient of "Top Editor" award for outstanding contributions to the IEEE TRANSACTIONS ON VEHICULAR TECHNOLOGY in 2011, 2014, and 2015. He is a Co-Chair of IEEE Intelligent Transport Systems Society Technical Committee on Communication Networks. He has served as a Chair, Co-Chair, and TPC member in a number of international conferences. He is a Fellow of IET.

J. Andrew Zhang (M'04–SM'11) received the B.Sc. degree from Xi'an JiaoTong University, Xi'an, China, in 1996, the M.Sc. degree from the Nanjing University of Posts and Telecommunications, Nanjing, China, in 1999, and the Ph.D. degree from the Australian National University, Canberra, ACT, Australia, in 2004. He is currently an Associate Professor with the School of Electrical and Data Engineering, University of Technology Sydney, Sydney, NSW, Australia. He was a researcher with Data61, CSIRO, Australia, from 2010 to 2016, the Networked Systems, NICTA, Australia, from 2004 to 2010, and ZTE Corp., Nanjing, China, from 1999 to 2001. He has authored/coauthored more than 130 papers in leading international journals and conference proceedings. His research interests are in the area of signal processing for wireless communications and sensing, and autonomous vehicular networks. He has won four Best Paper Awards for his work published in several international journals and conferences. He is a recipient of CSIRO Chairman's Medal and the Australian Engineering Innovation Award in 2012 for exceptional research achievements in multi-gigabit wireless communications.